Supporting Information

Lactonic sophorolipid increases surface wettability of poly-L-lactic acid electrospun fibers

Alexis M. Ziemba[‡1,3], Keith P. Lane[‡1,3], Bailey Balouch[‡1,3], Anthony R. D'Amato[1,3], Filbert Totsingan[2], Richard A. Gross[2,3], Ryan J. Gilbert[1,3*]

Affiliations: [1]Department of Biomedical Engineering and [2]Department of Chemistry and Chemical Biology, 110 8th Street, Rensselaer Polytechnic Institute, Troy, NY, 12180, USA; [3]Center for Biotechnology and Interdisciplinary Studies, 1623 15th Street, Rensselaer Polytechnic Institute, Troy, NY, 12180, USA

[‡]Indicates equal experimental, design, and writing contributions to the manuscript

Corresponding Author
*E-mail: gilber2@rpi.edu.

Pages: 10
Spectrum: 1
Figures: 1
Tables: 3

Materials and Methods

Materials Information

Table S1. Materials and product information

Material	Company	Location	Product #	Lot #
4′,6-diamidino-2-phenylindole	Thermo Fisher	Waltham, MA	62247	
Alexa Fluor 488 Phalloidin	Thermo Fisher	Waltham, MA	A12379	1885245
Bovine Serum Albumin (BSA)	Sigma-Aldrich	St. Louis, MO	A9647	SLBT4366
Chloroform	Fisher Scientific	Hampton, NH	C298-1	
Dulbecco's Modified Eagle Medium	Gibco	Gaithersburg, MD	12800-082	1973025
Ethylene Oxide	Anprolene	Haw River, NC	AN-73	
Fetal Bovine Serum	Gibco	Gaithersburg, MD	10437-028	1972428
Glutamax	Gibco	Gaithersburg, MD	35050-061	2037045
Hank’s Balanced Salt Solution	Gibco	Gaithersburg, MD	28372	
Human Foreskin Fibroblasts	ATCC	Manassas, VA	SCRC-1041	
Imaging Dish	Ted Pella	Redding, CA	14035-20	
Paraformaldehyde	Electron Microscopy Sciences	Hatfield, PA	15710	
Penicillin-Streptomycin	Gibco	Gaithersburg, MD	15140	2037045
Phosphate Buffered Saline	Thermo Fisher	Waltham, MA	28372	
Poly-L-lactic acid (PLLA)	NatureWorks	Minnetonka, MN	6201D	9051-89-2
TryplE Express	Gibco	Gaithersburg, MD	12605-028	2046796
Tween-20	Fisher Scientific	Hampton, NH	BP337-100	

Table S2. Equipment and software information

Instrument	Company	Location
DSC-Q100	TA Instruments	New Castle, DE
ImageJ	National Institutes of Health	Bethesda, MD
IX-81 Confocal Microscope	Olympus	Melville, NY
Metamorph Premier 7.7.3.0	Molecular Devices	San Jose, CA
Minitab Software	Pennsylvania State University	State College, PA
PixelLink Camera	PixelLink	Ottawa, ON
Technics Hummer V Sputter Coater	Anatech USA	Hayward, CA
Versa 3D Dual Beam Scanning Electron Microscope	FEI	Hillsboro, OR

Synthesis of lactonic SL 6',6"-diacetate [LSL(6'Ac, 6"Ac)]: The synthesis of the natural glycolipid starting material LSL was performed following literature methods published by Gross et al.[1,2] Briefly, fed-batch fermentation of *Candida Bombicola* ATCC 22214 inoculum aliquots (2–4×10^{11} cells per mL) was conducted maintaining the oxygen transfer rate between 50 and 80 mM O_2/L h^{-1}. The carbon sources were oleic acid (>95% purity) and glucose. Forty g of sunflower oil with high oleic acid content, 100 g of glucose, 10 g of yeast extract, and 1 g of urea in 1 L of water were used. The crude sophorolipids were extracted with ethyl acetate from the fermentation broth and dried under vacuum. The diacetylated lactonic sophorolipid, LSL, was separated from crude mixture either by flash chromatography using chloroform and methanol (10:1) or by recrystallization from ethyl acetate/hexane (1:1) (twice). This protocol provides product volumetric yields up to >300 g/L (productivity ~1.5 g/L h-1).

Yield = 85%; **Purity** = 98%; **Rf** [$CHCl_3$/CH_3OH 8:2] = 0.69; **^{1}H NMR** (500 MHz, DMSO-d_6): □ (ppm) 1.12 (3H, d, *J* = 6.5 Hz, -C*H*$_3$), 1.16-1.60 (20H, m, -C*H*$_2$-), 2.00 (10H, m, -C*H*$_2$CH=CHC*H*$_2$- and 2C*H*$_3$CO-), 2.30 (2H, t, *J* = 6.7 Hz, -C*H*$_2$COO-), 3.05-3.15 (2H, m, H-4' and H-2"), 3.24 (1H, t, *J* = 8.4 Hz, H-2'), 3.35-3,49 (3H, m, H-3', H-5' and H-3"), 3.60 (2H, m, H-17 and H-5"), 3.98 (2H, m, H-6"), 4.06 (1H, dd, J = 11.4 and 7.0 Hz, H-6'a), 4.22 (1H, dd, J = 11.9 and 2.1 Hz, H-6'b), 4.37 (1H, d, *J* = 7.7 Hz, H-1'), 4.51 (1H, d, *J* = 7.8 Hz, H-1"), 4.71 (1H, t, *J* = 9.5 Hz, H-4"), 5.27 (1H, d, *J* = 5.1 Hz, O*H*), 5.30 (4H, m, -C*H*=C*H*- and OHs), 5.43 (1H, br s, O*H*), 5.70 (1H, br s, O*H*) (Spectrum S1). **ESI-MS** (positive mode): m/z 711.0 ($M + Na^+$).

The purity was estimated from the integral ratio of the CH_2 protons signal (**2**) of ester (at 2.25 pm) and acid SL (at 2.16 ppm) (see below). Hence, the following equation was established:

$$Purity\ (\%) = \frac{I(proton\ 2)ester}{I(proton\ 2)ester + I(proton\ 2)acidic} \times 100 = \frac{I_{2.25\ ppm}}{I_{2.25\ ppm} + I_{2.16\ ppm}} \times 100$$

I = the integral area

Purity = 98%

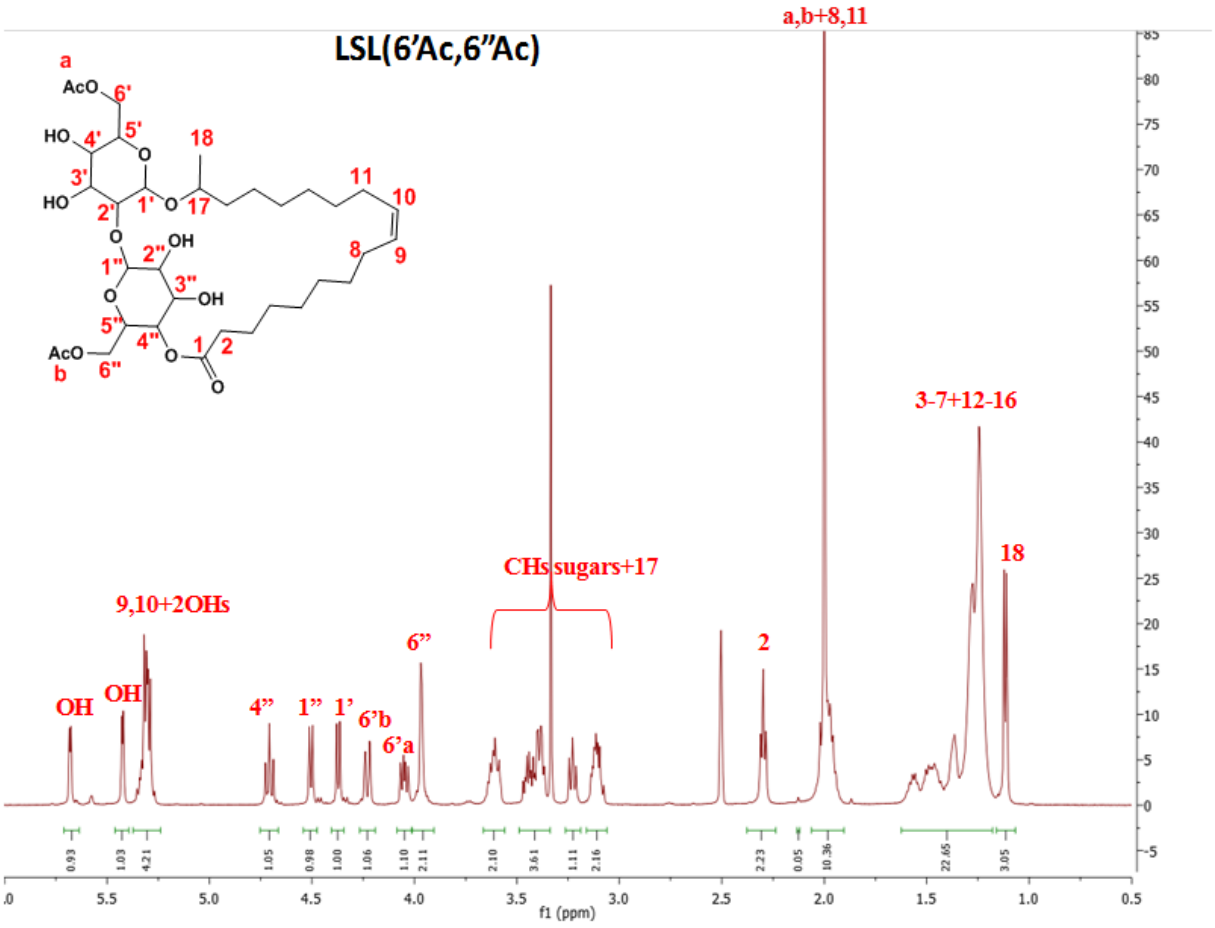

Spectrum S1. ^{1}H NMR spectrum of LSL taken with an Agilent 500 MHz in DMSO-d_6.

Electrospinning: Utilizing previously described techniques[3], solutions of PLLA and PLLA+LSL were electrospun into fiber scaffolds on 15 x 15 mm coverslips. LSL was synthesized in the Gross laboratory at Rensselaer Polytechnic Institute (please refer to Supporting Information). The PLLA fibers were electrospun onto coverslips using an 8% (wPLLA/w$CHCl_3$) solution in chloroform ($CHCl_3$). The fabrication parameters to produce PLLA fibers were as follows: 15 kV applied voltage, 1000 rpm mandrel rotation speed, 2.08 cc/h solution flow rate, and 21% relative humidity. LSL was added to PLLA in a 20% (wLSL/wPLLA) dry mixture. As the addition of small molecules can lower solution viscosity[4], the LSL-PLLA mixture was dissolved in chloroform (10% wPLLA /w$CHCl_3$). The fabrication parameters for PLLA + LSL fibers were as follows: 12.5 kV applied voltage, 1250 rpm mandrel rotation speed, 1.5 cc/h solution flow rate, and 21% relative humidity. The fiber collection time for both groups was 15 min to collect a single layer of fibers for characterization. Both types of fibers were placed in a vacuum overnight to aid in residual solvent removal[5]. A minimum of three batches of each fiber type were fabricated from independently prepared electrospinning solutions (n=3+).

Scanning electron microscopy: The electrospun fibers were sputter coated with approximately 0.5 nm of Au/Pd with a Technics Hummer V Sputter Coater. A FEI Versa 3D Dual Beam scanning electron microscope (SEM) was used to image the fibers with a working distance of 10 mm, spot size of 5.0, and an accelerating voltage of 2 kV. Five fields of view (in the center and near the 4 corners of each coverslip) were chosen at random to represent the entire population of fibers and imaged at 2000X magnification. Three independently fabricated batches of fibers were assessed (n=3).

Fiber characterization: SEM images were analyzed using ImageJ software. The diameter of each fiber was measured perpendicular to the length of the fiber using the line tool in ImageJ. The alignment of the fibers was found by drawing a line parallel to the length of each fiber and measuring the angle; all angles were normalized to the median angle of each field of view and plotted as a histogram of angle of deviations from the median angle. The fiber surface coverage was calculated by multiplying the average fiber diameter of the field of view (FOV), the number of fibers in a field of view, and fiber length and then dividing by the total area of the field of view (equation below).

$$\%\, Surface\ Coverage = \frac{average\ fiber\ diamter\ for\ FOV\ \times number\ of\ fibers\ in\ FOV\ \times fiber\ length}{area\ of\ FOV}$$

Film fabrication: To show whether changes in fiber wettability were due to differences in hydrophobicity of PLLA and LSL, we first measured the contact angle of PLLA-only and LSL-only films. To fabricate these films, PLLA (4% w/w) and LSL (10% w/w) were dissolved in $CHCl_3$ then drop cast onto 15 x 15 mm glass coverslips. For fibroblast adhesion tests, PLLA films were fabricated as described above. To fabricate PLLA+LSL films, 20% wLSL/wPLLA dry mixture was dissolved in $CHCl_3$ (4% wPLLA+LSL/w$CHCl_3$). Solution was then drop cast onto 15 x 15 mm glass coverslips. A minimum of n=3+ technical replicate films for each condition were fabricated.

Contact Angle: Coverslips with either fiber mats or drop cast films were placed in between a PixelLink camera with a Nikon lens and incandescent light source with fibers oriented towards the camera. A droplet of distilled water (45 µL) was deposited onto the films and fibers, and images were captured. Due to fiber alignment, images of the droplets down the length of the fibers were used. The contact angle at the liquid-vapor and solid-liquid boundaries was analyzed with the angle tool in ImageJ. A minimum of three films and three coverslips with independently-fabricated batches of fibers were assessed for each material condition (n=3+).

Differential Scanning Calorimetry (DSC): PLLA and PLLA+LSL fibers (5 mg) were hermetically sealed in aluminum sample pans. Fiber samples were placed in the heat exchange apparatus of a TA instruments DSC-Q100. Samples were heated from 20°C to 180°C then cooled to 20°C, incrementing temperature by 10°C/min, as described previously[5]; this cycle was repeated three times. The heating and cooling cycles

were analyzed using TA Universal Analysis Software, which yielded the thermal properties of the fibers: glass transition temperature (T_g), melting temperature (T_m), crystallization temperature (T_c), heat of fusion (ΔH_m), and percent crystallinity (χ_c). Each fiber type had three separate fiber batches analyzed (n=3).

Fibroblast Culture: Prior to cell experiments, films and fibers were sterilized using ethylene oxide and allowed to air out for a minimum of 24 h. Human Foreskin Fibroblasts (HFF-1) were cultured in cell culture medium containing Dulbecco's Modified Eagle's Medium containing Fetal Bovine Serum (10%), Glutamax (1%), and Penicillin-Streptomycin (1%). Cells were maintained at 37°C and 5% CO_2 in a cell culture incubator. Cells were lifted from tissue culture flasks with TryplE Express and counted using a hemocytometer. Prior to plating for adhesion experiments, PLLA and PLLA+LSL film and fiber scaffolds were equilibrated by bathing in 1 mL of cell culture medium in a 12-well tissue culture plate for 15 min. Fibroblasts were seeded onto each scaffold (a minimum of n=3 per material condition) directly at 100,000 cells in a volume of 1 mL culture media. Scaffolds were incubated for 30 min to allow fibroblasts to adhere, at which point scaffolds were washed with Hank's Balanced Salt Solution (1 mL) to remove non-adherent cells. Scaffolds with adherent cells were incubated for 24 h in fresh cell culture medium before fixation with paraformaldehyde for staining.

Fibroblast Staining: Fibroblasts adhered to material scaffolds were fixed with paraformaldehyde (4% v/v in phosphate buffered saline (PBS)) for 10 min. To label F-actin throughout the cell, fibroblasts were stained with Alexa Fluor 488 Phalloidin (1:1000) diluted in 1% bovine serum albumin and 0.1% Tween-20 in PBS for 90 min. Following incubation, phalloidin solution was removed, and cells were counterstained by incubating with 4′,6-diamidino-2-phenylindole (DAPI; 1:1000) in PBS for 10 min. Scaffolds were then washed three times with PBS.

Fluorescence Microscopy: Confocal images were acquired using an Olympus IX-81 Confocal Microscope and Metamorph Premier 7.7.3.0. Scaffolds were inverted and placed in an imaging dish prefilled with PBS. The stage position was preset to acquire at least 12 images per coverslip, moving clockwise in a square around the center of the coverslip, to survey the scaffold while avoiding the center and edges. A Z-series at each stage position was acquired at 10X magnification using green fluorescent protein (GFP; λ_{ex}488/ λ_{em}510) and DAPI (λ_{ex}358/ λ_{ex}461) fluorescence channels to image Phalloidin and DAPI, respectively.

Fibroblast Adhesion Analysis: To prepare images for analysis, each Z-series was collapsed by creating projections using the maximum intensity pixels, and GFP and DAPI channel images were merged together. The number of cells adhered to each material scaffold was determined by counting the number of cells per field of view (0.67 mm^2). Any visible object that was positively labeled with both Phalloidin and DAPI was counted as a cell. Images that were out of focus or did not contain any cells were excluded from analysis. A minimum of 117 cells were counted on each material condition.

Statistical Analysis: Minitab was used to perform statistical analyses. All data were first tested for normality using the Ryan-Joiner method. As diameter data were not normally distributed, medians and interquartile ranges (IQR) were found by combining the average diameter measurements for each field of view; the diameter data were then represented as a plot of boxplots. Histograms depicting angle deviations from the median fiber angle were used to visualize distributions of the alignment of the fiber types. The median angle of deviation was used to compare the difference in fiber alignment between groups. Mean fiber density (and standard deviation) was calculated using a weighted average based on the number of fibers from each batch. Data were plotted as a mean ± standard deviation. For diameter, alignment, and density assessments, a Kruskal-Wallis test was used to assess significance between groups with a statistical significance threshold of $\alpha \leq 0.05$. Data recorded for contact angle and DSC data were averaged for each fiber type. A two-tailed *t*-test was performed to check the significance between the groups for all contact angle and DSC tests; the statistical significance threshold was set to $\alpha \leq 0.05$. As fibroblast adhesion data were not normally distributed, data were represented as a plot of boxplots. Welch's ANOVA with a post hoc Games-Howell

test was used to assess significance with a threshold of $\alpha \leq 0.05$. The 95% confidence intervals were also computed to support the Welch's ANOVA analysis.

Results information

Sample DSC Curves

We graphically displayed the first and second heating cycles and the first cooling cycle to learn more about the localization of LSL within the fibers (Figure S1). Through the first DSC cooling cycle, PLLA exhibited recrystallization at ~100°C (Figure S1B). For the second heating cycle, a very minimal crystallization peak was observed upon heating PLLA (Figure S1C). We observed an absence of recrystallization during the first cooling cycle for PLLA+LSL fibers (Figure S1B). Unlike PLLA fibers, we observed a substantial crystallization peak when the PLLA+LSL fibers were heated a second time (Figure S1C). These results further support that LSL nucleates PLLA crystallization.

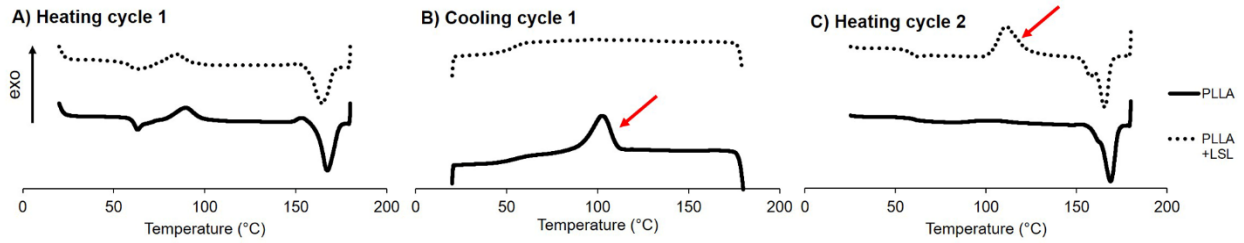

Figure S1. PLLA and PLLA+LSL fibers exhibit different recrystallization characteristics. Sample DSC cooling curves for PLLA (solid black) and PLLA+LSL fibers (dotted black) were A) heated from 20°C to 180°C, B) cooled from 180°C to 20°C, C) then heated again from 20°C to 180°C at a rate of 10°C/min. Red arrows indicates crystallization.

Additional Statistical Information for Fibroblast Adhesion Analysis

To further support differences in adhesion between material types, we compared the confidence intervals of the number of cells adhered on each material type. The lack of overlap between PLLA films and all other groups further supports the difference between the groups (Table S3).

Table S3. The 95% confidence intervals for fibroblast adhesion on the different material types.

Factor	N	Mean	St Dev	95% CI
PLLA Film	32	5.49	3.135	(4.32, 6.58)
PLLA+LSL Film	66	8.99	9.75	(6.59, 11.38)
PLLA Fibers	32	18.35	7.76	(15.55, 21.15)
PLLA+LSL Fibers	33	18.97	6.86	(16.53, 21.40)

References

(1) Felse, P.; Shah, V.; Chan, J.; Rao, K.; Gross, R. Sophorolipid Biosynthesis by Candida Bombicola from Industrial Fatty Acid Residues - ScienceDirect. *Enzyme and Microbial Technology* **2007**, *40* (2), 316–323.

(2) Guilmanov, V.; Ballistreri, A.; Impallomeni, G.; Gross, R. Oxygen Transfer Rate and Sophorose Lipid Production by Candida Bombicola. - PubMed - NCBI. *Biotechnology and Bioengineering* **2002**, *77* (5), 489–494.

(3) Wang, H. B.; Mullins, M. E.; Cregg, J. M.; Hurtado, A.; Oudega, M.; Trombley, M. T.; Gilbert, R. J. Creation of Highly Aligned Electrospun Poly-L-Lactic Acid Fibers for Nerve Regeneration Applications. *J. Neural Eng.* **2009**, *6* (1), 016001.

(4) Johnson, C. D. L.; D'Amato, A. R.; Gilbert, R. J. Electrospun Fibers for Drug Delivery after Spinal Cord Injury and the Effects of Drug Incorporation on Fiber Properties. *Cells Tissues Organs (Print)* **2016**, *202* (1–2), 116–135.

(5) D'Amato, A. R.; Bramson, M. T. K.; Corr, D. T.; Puhl, D. L.; Gilbert, R. J.; Johnson, J. Solvent Retention in Electrospun Fibers Affects Scaffold Mechanical Properties. *Electrospinning* **2018**, *2* (1), 15–28.